TAC-0/237
For Author's Correction Only

Theor. Appl. Climatol. 000, 1–19 (2006)
DOI 10.1007/s00704-006-0237-5

Theoretical and Applied Climatology
Printed in Austria

[1] Department of Environmental Dynamics and Bioclimatology, University of Łódź, Łódź, Poland
[2] Department of Meteorology and Climatology, University of Łódź, Łódź, Poland

Jet stream patterns over Europe in the period 1950–2001 – classification and basic statistical properties

J. Degirmendžić[1] and **J. Wibig**[2]

With 10 Figures

Received September 20, 2004; revised February 2, 2006; accepted March 10, 2006
Published online • •, 2006

Summary

Primary goal of presented study is to classify the most frequent patterns of the upper tropospheric jet stream over Europe. Wind fields were grouped into separated classes with the help of the correlation-based Lund's technique. The treatment of vector fields with Lund's method was achieved by replacement linear Pearson coefficient with vector correlation coefficient. The outstanding features of the upper-level circulation and ground-based weather associated with each jet type were analysed. Finally, basic statistics of jet stream patterns (frequency, duration time, day-to-day changes of jet structure) as well as their trends were estimated. The analysis was conducted on the basis of mean daily wind components at 200 hPa level, air temperature at 850 hPa, sea-level pressure, vertical velocity and geopotential at 500 hPa level. Data set was extracted from the NCEP/NCAR Reanalysis. The warm half-year in the period 1950–2001 was taken into consideration. The first 15 most frequent jet types, including 60.8% of the sample, were selected. Three jet stream types (C, E and I) are associated with distinct temperature changes in western Europe. Another three types (B, F and O) cause significant thermal advection in eastern and central Europe. Seasonal differences in frequency and duration time of jet stream patterns are also observed. Meridional types (A, C and D) dominate in spring, while in summer, patterns with intensified zonal flow prevail (B, E and J). At last, it is worth noticing that the majority of selected jet types pronounce an increase in day-to-day changes of wind field, which may indicate slight enhancement of circulation dynamics in the upper troposphere.

1. Introduction

Upper tropospheric jet stream constitutes a significant factor influencing physical processes in the lower atmosphere, both in synoptical and climatological time scales. Jet stream modifies its associated divergence field (Ziv and Paldor, 1999), alter the intensity of vertical drafts in the vicinity of jet streaks enhancing or suppressing cyclogenesis (Rose et al., 2004) and steer the weather patterns (Trenberth, 1991). Despite its fundamental role in constituting the weather and climate, still there is lack of the composite analyses which average characteristic atmospheric states according to various jet patterns. This is the task for a regional synoptic climatology. On the other hand, there are plenty of papers comparing the mean state of the atmosphere with mean jet stream position, which is characteristic of the classical climatology approach (Reiter, 1963). Similarly, case studies analysing extreme weather phenomena and their relationship with jet stream dynamics are rather frequent (e.g. Uccellini and Kocin, 1987; Uccellini et al., 1984). The main inhibitor for the development of jet stream synoptic climatology is the absence of jet stream classification. Although there are several works concerning jet stream spatial structure, they are confined only to the limited geographical areas, e.g.: Croatia and Bosnia (Malnar-Tomic, 1995), Turkey (Erdogmus, 1992), the Middle East (Singh, 1980), Germany (Kasper, 1976, 1978) and Poland (Budziszewska, 1977). The structure of the split jet over the UK was investigated by Shutts (1987).

Study described here has a few principal objectives. The first is to test the application of Lund's method to vector fields. The other are: to distinguish the dominating jet stream patterns over Europe, to characterise the most outstanding features of upper-level circulation and ground-based weather related to selected jet types and to estimate the basic statistical properties of jets, such as frequency of their occurrence, duration, day-to-day changes of the jet structure and long-term trends of these statistics.

2. Data and methods

To identify the jet stream on upper maps Glickman criterion was applied: "jet stream is indicated wherever it is reliably determined that the wind speed equals or exceeds 50 knots ($\sim 26\,\mathrm{ms}^{-1}$)" (Glickman, 2000). Classification of jet stream patterns was based on mean daily wind components at 200 hPa isobaric level. The frequency of blocking associated with each jet stream class was evaluated by means of Lejenäs-Økland index. *LO* index is defined as:

$$LO(\lambda) = Z(40^\circ\,\mathrm{N}, \lambda) - Z(60^\circ\,\mathrm{N}, \lambda),$$

where $Z(\varphi, \lambda)$ is the daily mean geopotential height of 500 hPa surface in the point of geographical coordinates φ and λ (Lejenäs and Økland, 1983). This index was calculated for meridians ranged from 20° W to 50° E with a step of 2.5°. Relative frequency of blocking, i.e. the number of days with $LO < 0$ with respect to the total number of cases in a given group was estimated.

The analysis of the lower tropospheric state, representative for the jet stream classes was based on air temperature at 850 hPa level, sea-level pressure and vertical velocity at 500 hPa. Composites of these parameters accounting for all class members were constructed. Differences between composite fields and long-term average were tested with the t-statistic. The dataset used in this study was the NCEP/NCAR gridded reanalysis, described in detail by Kalnay et al. (1996). Area limited by parallels 30 and 70° N and meridians 20° W and 50° E with grid resolution $2.5^\circ \times 2.5^\circ$ was analysed. Analysis spans the period 1950–2001 and warm half-year (Apr–Sep).

There are many methods of identifying spatial patters like: clustering procedures (Kalkstein et al., 1987), empirical orthogonal functions (von Storch and Zwiers, 1999; Wibig, 2001), Kirchhofer's technique (e.g. Kaufmann et al., 1999) and artificial neural network approach (e.g. Bolek and Degirmendžić, 2004). However, these methods are usually applied to scalar fields such as geopotential height or air temperature. Vector fields are considered rarely. Hardy and Walton (1978) provided statistical background for EOF treatment of two-dimensional vector fields. Legler (1983) applied EOF technique to analyse wind vectors variability. Apart from these sophisticated statistical techniques there are also correlation-based methods. They are very simple from mathematical point of view and give similar results (Richman, 1981; Reap, 1994).

In order to classify jet stream patterns such correlation-based method (also known as Lund's method) was used in this study (for a detailed description see Lund, 1963). Lund presented a very simple procedure of field classification taking advantage of Pearson's linear correlation coefficient. This method preserves the image of the field structure. Furthermore, the input dataset consists of observed fields of an analysed element and the output gives the most frequently observed fields of this element (Bischoff and Vargas, 2003). It makes the clear-cut interpretation of the results possible.

To apply Lund's technique to vector fields, the linear correlation coefficient was replaced with the vector correlation coefficient $\rho_v{}^2$ proposed by Crosby et al. (1993). The vector correlation coefficient varies between 0.0 (no correlation) and 2.0 (perfect correlation). Instead of taking into consideration vector time series, which was done by Breaker et al. (1994), spatial records of vectors from all 493 grid points of two wind fields were correlated.

Important parameter that must be set a priori (i.e. before the analysis) is the correlation threshold. The higher the threshold value, the smaller percent of daily fields classified and the larger the number of patterns. Low threshold value results in a small number of classes but internal diversity within each of them is relatively high. The threshold correlation applied to scalar fields usually ranges from 0.7 to 0.9 (Huth, 1996). Unfortunately no hints are provided in the literature as regards vector correlation threshold. In this study the percentile 95 of the set of 45, 272, 370 correlation coefficients, describing the similarity of each pair of 9516 daily fields, was set as a threshold value. It equals 0.66.

To classify the jet stream patterns a correlation coefficient is calculated for each pair of the daily maps. Basing on the coefficients greater than or equal to the threshold value, days defining types and groups of days with wind patterns similar to defined ones are identified. The answer to the question of how many "typical patterns" should be retained is attempted by several authors but the nature of their decision is always arbitrary. Reap (1994) selected only classes which contained more than 3% of the total sample. Paegle and Kierulff (1974) decided that the last circulation type must consist of at least 15 cases (1.2% of the sample). Overland and Hiester (1980) designated that a type must have minimum 10 members (2.8% of the sample). The last type selected by Lund (1963) consists of 1.8% of the sample. Bischoff and Vargas (2003) set 5% frequency threshold. In this analysis minimum size of the jet stream class equals 1.5% of the total sample. Under such criterion 15 types of jet stream were distinguished. They constitute 60.8% of all cases (Fig. 1).

In order to evaluate the similarity of wind fields grouped into the same class, the stability of wind direction in each grid point within the borders of the analysed area was calculated. The index of directional stability is defined by the formula:

$$P_k = \frac{\left\| \sum_{i=1}^{n} \overrightarrow{W}_{k,i} \right\|}{\sum_{i=1}^{n} |\overrightarrow{W}_{k,i}|} \times 100$$

where the numerator is the speed of the resultant wind calculated from the wind vectors in grid point k on the day i. The summation is carried out for all days (n) grouped into a given jet stream class. The denominator is the sum of wind speed values on the same days (Panofsky and Brier, 1958). Index P_k holds within the range 0–100%. 0% indicates that wind is equally likely from all directions or blows half the time from one direction and half the time from the opposite. 100% means that the wind direction in all days with the given pattern is precisely the same. The spatial distribution of the P_k informs about the similarity of the vector fields joined into the same class and also helps to evaluate how well the distinguished jet stream type represents the whole group. Special attention was paid to P_k calculated for the jet stream structure, i.e. for the region where wind speed is higher than $26\,\mathrm{ms}^{-1}$.

The following statistics were computed for each jet stream class:

1. The frequency of jet type occurrence in each month and the whole warm season in the period 1950–2001.
2. Mean duration time of jet stream pattern [days] – average length of all groups composed of the consecutive fields that belong to the same class and form continuous time sequence uninterrupted by other jet type. Groups placed symmetrically at the turn of two months were not taken into account while calculating mean monthly duration. They entered analysis only when the whole half-year period was concerned. The groups beginning on the 1st of April and ending on the 30th of September were omitted.
3. The maximum duration time of jet stream pattern [days] – the longest group described in point 2 that was observed in the period 1950–2001, calculated separately for each month and for warm half-year as a whole.
4. Mean day-to-day changes of the wind field – average vector correlation coefficient computed for each pair of consecutive fields included

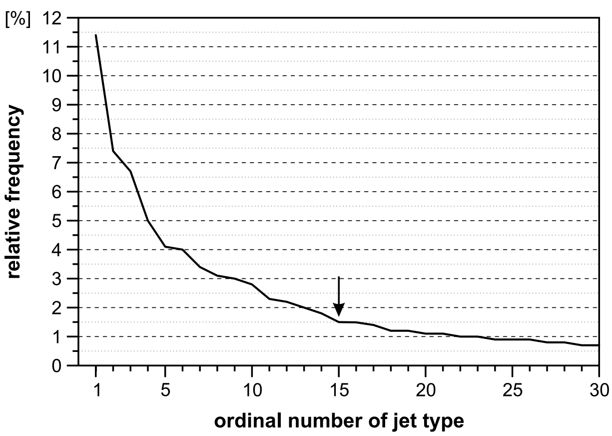

Fig. 1. The relative frequency of jet stream types in the warm half-year during the period 1950–2001. The arrow denotes the last, 15th type that is retained

in the same jet stream category. Jet patterns lasting one day were automatically excluded from the analysis. Low (high) coefficient indicates high (low) day-to-day changes of jet stream structure. This statistic was calculated only for the warm half-year as a whole.

The linear trends of monthly means and values averaged for warm half-year of the above-mentioned statistics were estimated. Trends in frequencies of jet classes were calculated on the basis of 52-element records (with some values equal to 0). However, in the case of duration time and day-to-day changes, the lack of jet in particular year excluded this year from the analysis and the records were usually shorter than 52 (see Tables 4 and 5).

3. Description of jet stream patterns

Below, short characteristic of each of the first 15 most frequently occurring jet stream types is provided.

The A pattern is characterised by a well developed subtropical branch of jet stream, stretched

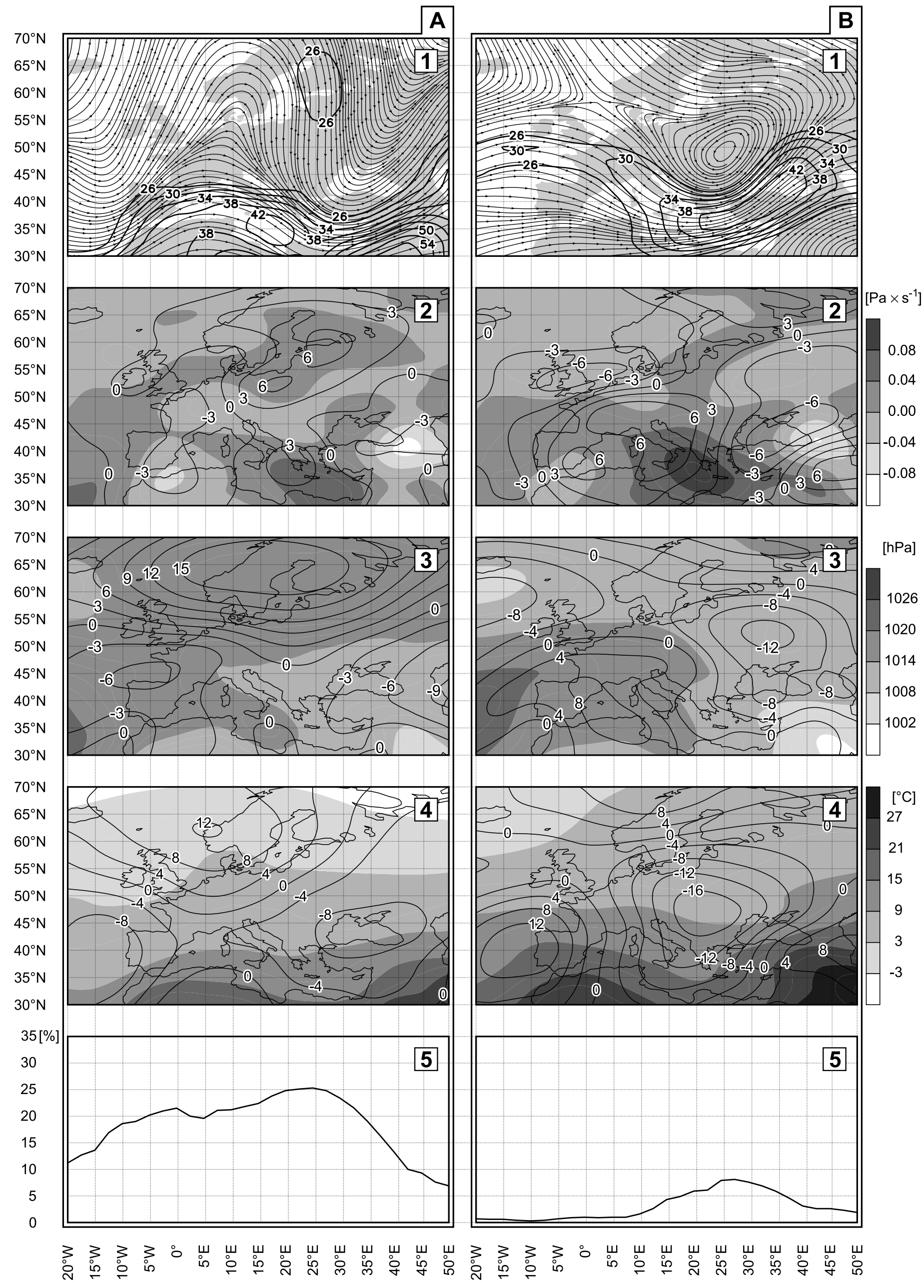

Fig. 2. Types A and B of jet stream – streamlines and isotachs greater than $26\,\mathrm{ms}^{-1}$ are depicted (1), associated composite fields of: vertical velocity at 500 hPa level (2), sea-level pressure (3), air temperature at 850 hPa level (4) and the number of blocks ($LO < 0$) related to the total number of class members (5). Note that on maps 2–4 composites are shaded and contours show distribution of t-statistic that asses statistical significance of differences between composite and long-term mean. $|t| > 2.57$ delimits areas where composites differ from the mean at $\alpha = 0.01$

over the Mediterranean and northern Africa. The wind speed in this branch reaches $58\,\mathrm{m\,s^{-1}}$. The polar jet stream, which exists in the form of a jetlet, is situated over Finland and embedded in the eastern part of the ridge over western Europe. Wind velocity in this region slightly exceeds $26\,\mathrm{m\,s^{-1}}$. Over the Baltic basin descending motions dominate. Vertical velocity, averaged for the whole class, is in the order of $0.02\,\mathrm{Pa\,s^{-1}}$ in this area. This value differs significantly from the long-term average. The strongest ascending draft ($-0.08\,\mathrm{Pa\,s^{-1}}$) is formed to the south-east of the Black Sea. It is possibly associated with a divergence in the left exit quadrant of the subtropical jet streak. Sea level pressure field is dominated by anticyclone over Scandinavia and Azores high, which is shifted considerably westward. The Middle East is under the influence of the north-westerly extension of Pakistan low. As a result of such pressure distribution warm advection occurs in north-western Europe being especially strong in western Scandinavia. Southern part of the continent reveals cooling tendencies. Type A is a blocking one – 25% of daily

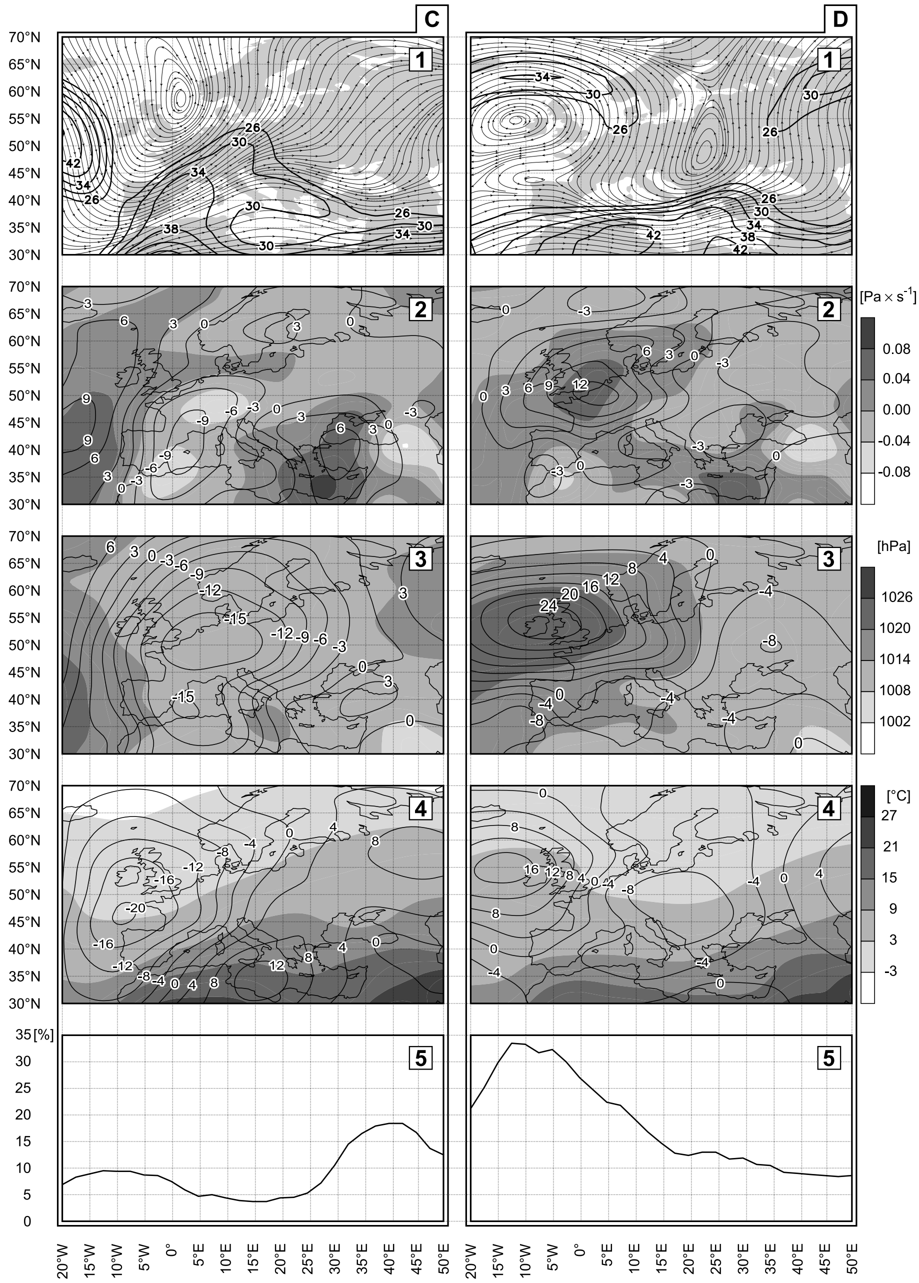

Fig. 3. Same as Fig. 2 except for types C and D

fields, members of A class, are characterised by the blocking circulation between 20 and 25° E meridians (Fig. 2).

The B pattern is represented by a wave-like jet stream with a jet streak situated in the eastern part of the trough over the Anatolian Peninsula. The maximum wind speed in the jet axis reaches $45\,\mathrm{ms}^{-1}$. Such position of jet streak relative to trough axis usually results in its filling up. On average, updrafts are observed over eastern Europe, enhanced beneath the delta region of upper jet with value equalled $-0.08\,\mathrm{Pa\,s}^{-1}$. Pressure in this region falls below the long-term mean. The largest drop is observed to the north of the Black Sea. Low pressure prevails also over north-western Europe. In the south-western part of the continent anticyclonic wedge spreading towards central Europe is observed. As a result, zonal flow is amplified in the lower atmosphere, especially between 45 and 55° N, which causes cooling, the most intense in central Europe. Warming is observed to the west of the Iberian Peninsula (Fig. 2).

The C jet stream pattern is characterised by a deep trough extended over the North Sea and

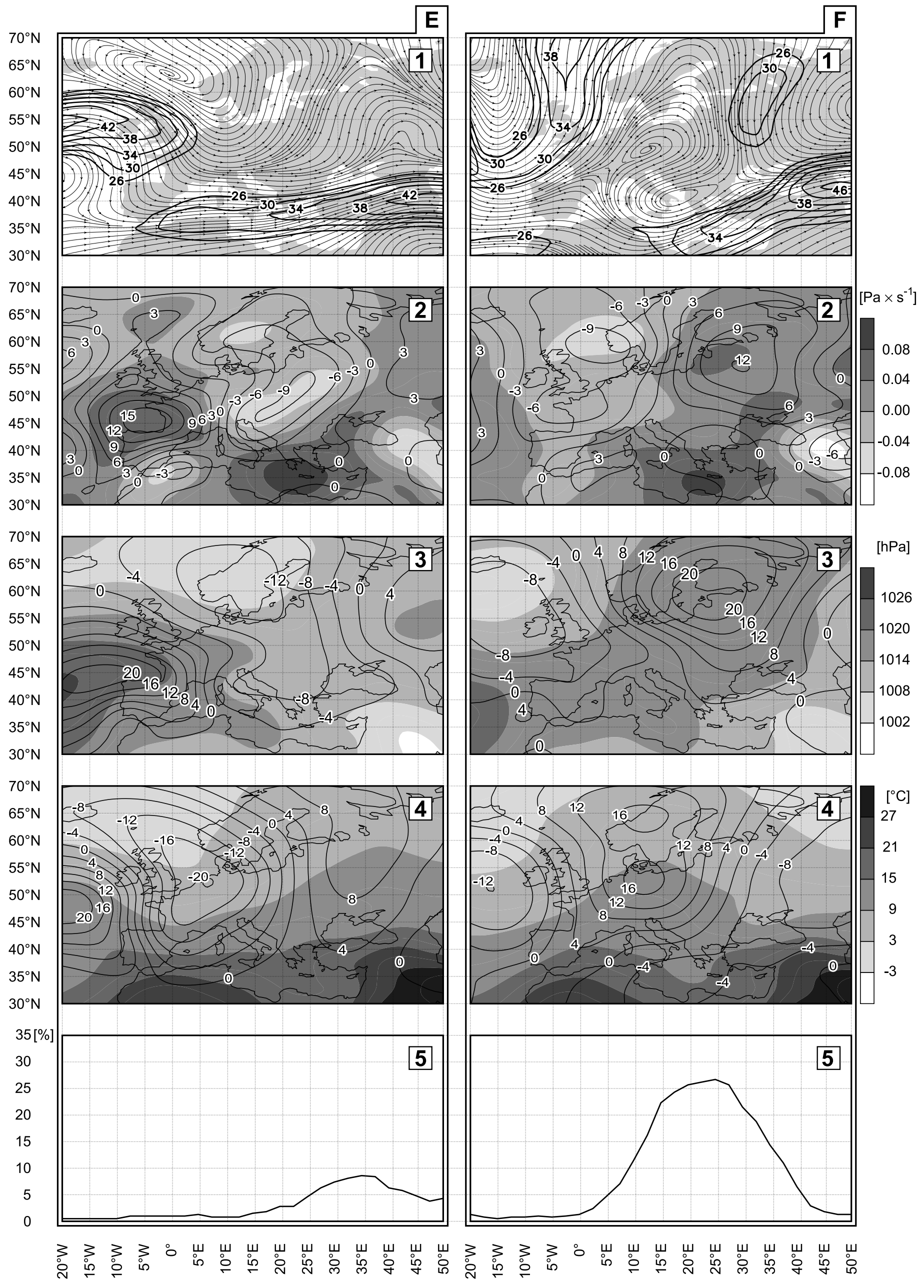

Fig. 4. Same as Fig. 2 except for types E and F

eastern Atlantic. The belt of ascending motions spreading from north-western African coast towards central-western Europe is typical for this pattern. Downdrafts are observed over the eastern Mediterranean and the Black Sea. Pressure field is dominated by cyclone developed over western Scandinavia and the North Sea. In its western part strong advection brings cold air down to the Iberian Peninsula and Africa (Fig. 3).

The main feature typical for the D pattern is upper anticyclone in the proximity of Ireland, which together with the trough over the Bay of Biscay forms so-called Rex block. Northern advection over central Europe is also associated with cut-off upper tropospheric low spreading over south-eastern Europe. In the northern sector of the anticyclone jet stream with a weak, anticyclonically curved jet maximum is located. Beneath right exit region descending motions are clearly visible, whereas over eastern Europe ascent prevails. Vertical motions are associated with pressure rise over the British Isles and pressure falls over south-eastern Europe and the Middle East. This type brings about low temper-

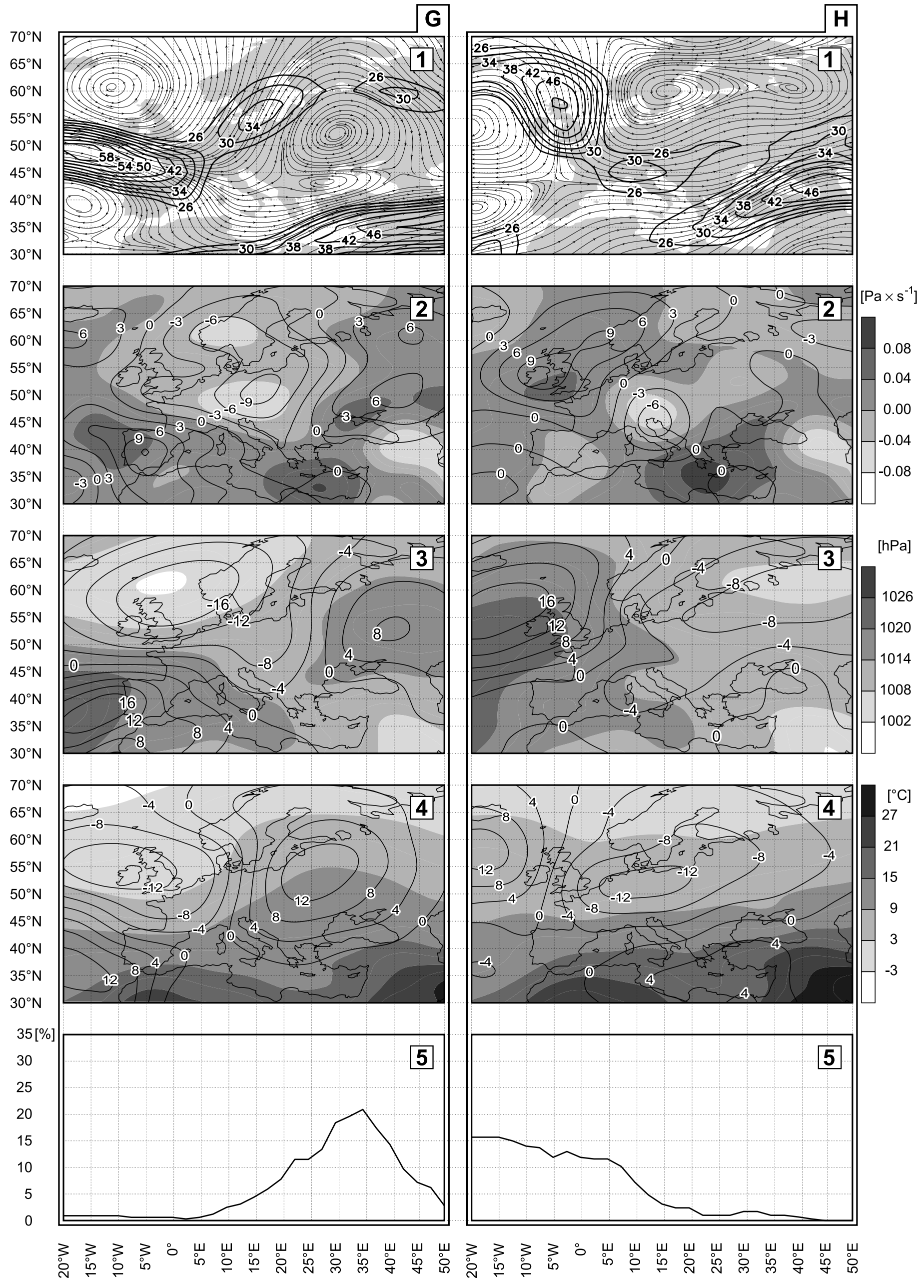

Fig. 5. Same as Fig. 2 except for types G and H

atures in central Europe and relatively warm weather in eastern Atlantic. It is connected with high frequency of blocking (up to 35% between 15–10° W) over the eastern sector of the North Atlantic and western Europe (Fig. 3).

The E jet stream type is an example of zonal flow. A weak tendency to blocking is marked only in the zone between 30 and 50° E. The air sinks beneath the right delta region of anticyclonically curved polar jet streak in the vicinity of the Bay of Biscay. Over the central part of the continent ascending motions prevail. As a result, Azores high is displaced to the north and influences western Europe while eastern and central Europe is covered with low pressure trough. This type intensifies north-westerly advection of cold and humid polar air over the British Isles and central-western Europe (Fig. 4).

The next pattern (F) is an example of Rex block formed by two cut-off pressure systems. The distribution of vertical velocity constitutes the classical example of the upper-ridge associated circulation – beneath its westward side ascent is observed and downstream from the

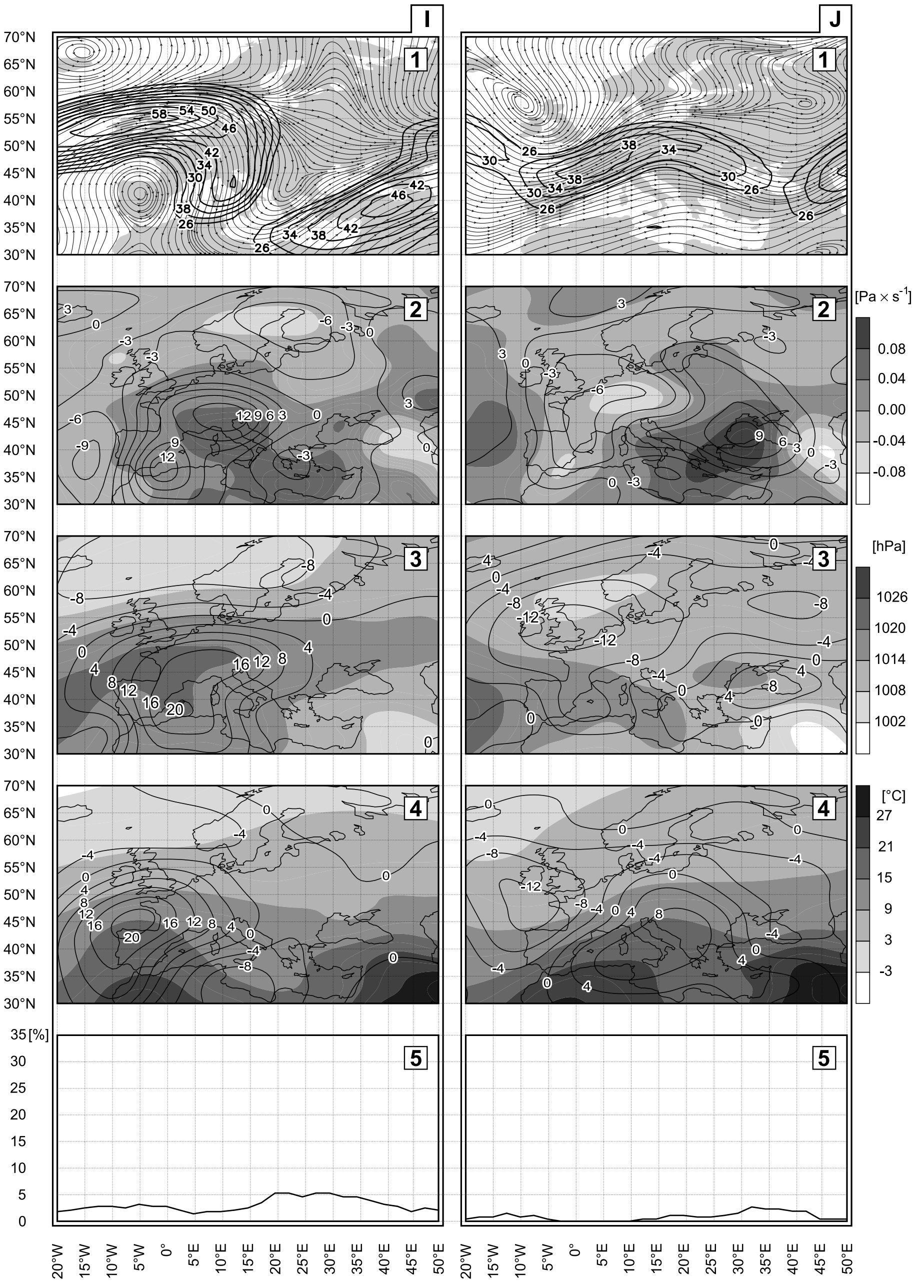

Fig. 6. Same as Fig. 2 except for types I and J

crest of the ridge the air sinks. Sea-level pressure is characterised by a dipole with the high pressure over the Baltic region and well developed Icelandic low. The most outstanding feature of temperature field is the advection of warm air crossing central Europe towards the north edges of the continent. Cooling affects only eastern Atlantic and, to a minor degree, also the Balkan Region due to the local advection of cold air. This advection is separated from the main cold air stream over eastern Europe (Fig. 4).

The G pattern is characterised by the strong jet stream with a maximum speed of $58\,\mathrm{ms}^{-1}$ over eastern Atlantic. It splits in the region of a diffluent block situated over eastern Europe. Northern branch crosses Scandinavia. Southern branch joins the subtropical jet. Two maxima of ascent seem to be associated with the right entrance and left exit sector of jet streak situated over the Baltic basin. Descending motions dominate over the Iberian Peninsula. The most significant positive anomalies are superimposed

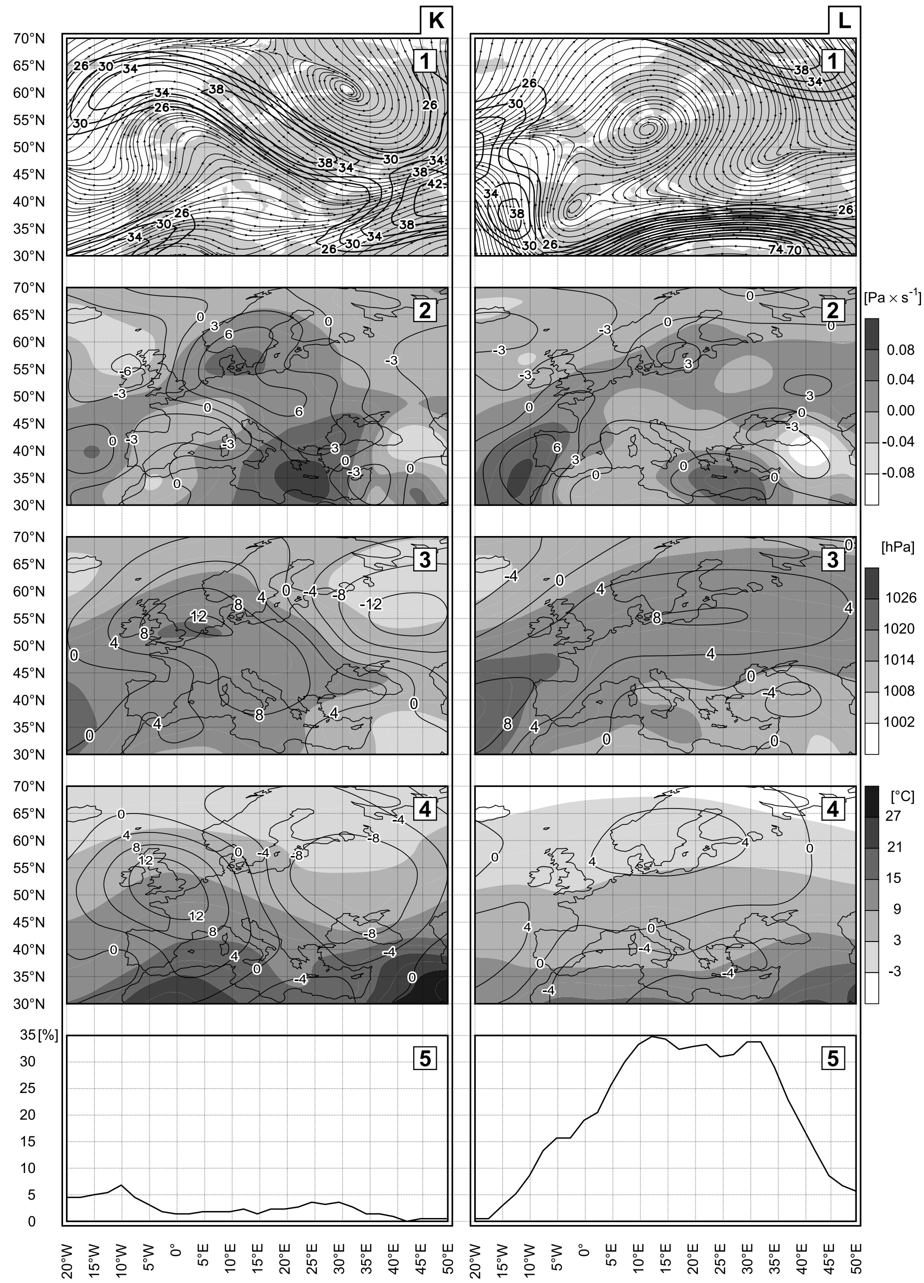

Fig. 7. Same as Fig. 2 except for types K and L

vertically with right exit region of eastern Atlantic jet streak. Air flow in the lower troposphere is typical for NAO positive phase. In western Europe strong zonal circulation is accompanied by cooling. Eastern part of the continent experiences warmer weather under the influence of East European high (Fig. 5).

The H type of jet stream is associated with the negative NAO phase – there is a considerable frequency of blocks in 20–10° W sector. Surface high pressure area covers north-eastern Atlantic while the low pressure system spreads over north-western Russia. Such circulation dipole intensifies the advection of cold air from the Norwegian Sea over western and central Europe. Southern Europe and the eastern Mediterranean experiences relatively warm weather (Fig. 5).

The wind speed in the jet streak over the Atlantic characteristic for type I equals $60\,\mathrm{ms}^{-1}$. This relatively high speed may be the symptom of the enhancing thermal contrast in September between the polar air and still warm subtropical air masses in the south. Significant enhancement of downdraft intensity is observed on the anti-

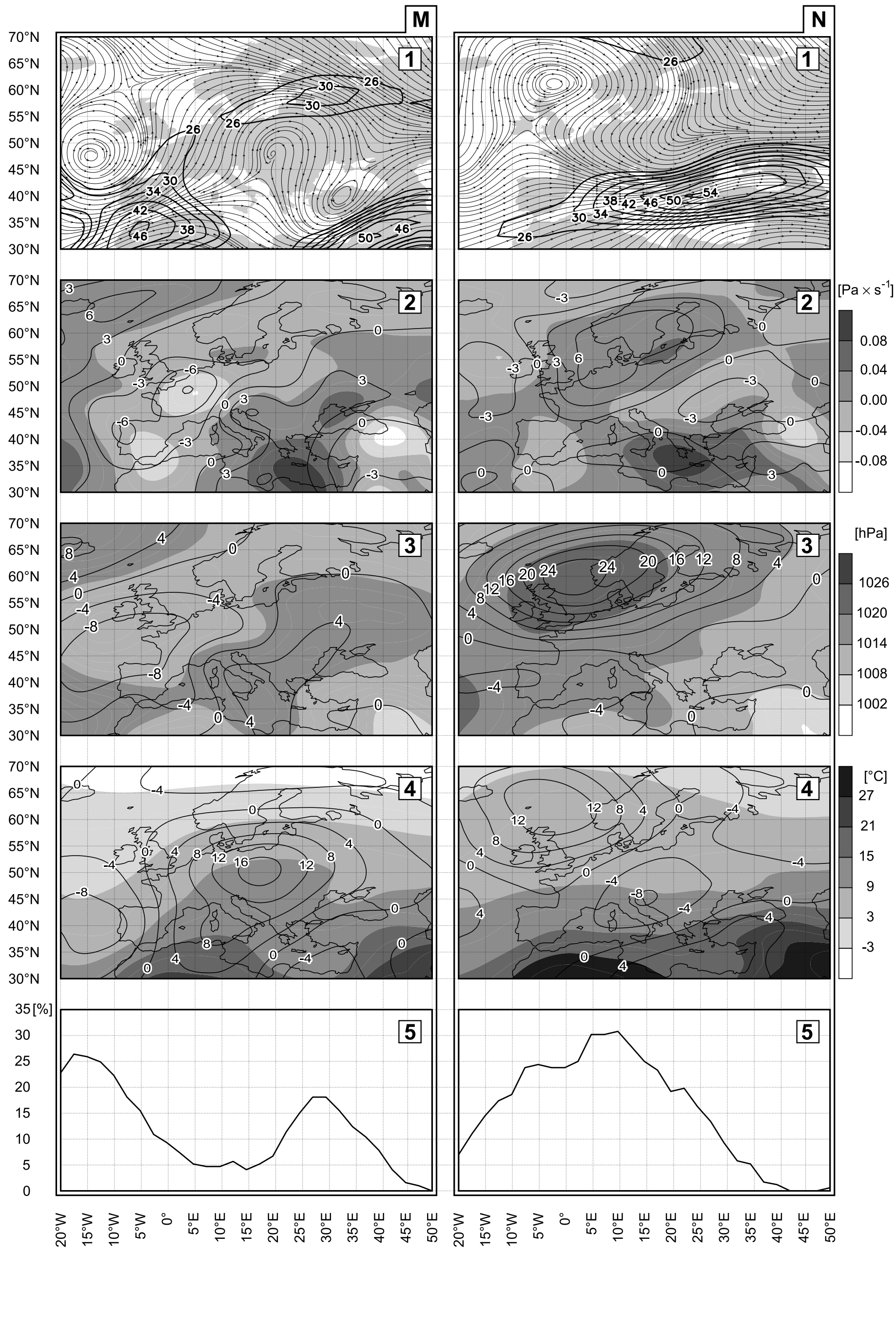

Fig. 8. Same as Fig. 2 except for types M and N

cyclonic side of the polar jet – over the Alps and the western Mediterranean. This amplifies Azores high wedge extended towards central Europe. Strong diffluent flow is present over the northern part of the Baltic basin which may force the air to rise and produce pressure falls beneath. Therefore Icelandic low is elongated towards Scandinavia. Significant warming is found over the Iberian Peninsula and cooling over the central Mediterranean (Fig. 6).

In case of type J, jet streak is situated downstream from the base of the upper trough over France. Thus, wave-like pattern may become less amplified with time and trough will lift out in the north-easterly direction. Close to the right exit region of the jet, i.e. to the south-west of the Black Sea, strong sinking motions are developed, equal to $0.1\,\mathrm{Pa\,s^{-1}}$. Also local pressure rise is observed in this region. Less intensive ascent is localised over western Europe that is to the south of low pressure system anchored over Scandinavia and the North Sea. The position of this low forces air masses to flow from north-west in western Europe and from south-west in eastern region. Consequently, low-level thermal advection produces cooling in western and warming in southern and central Europe. In general, strong zonal flow is characteristic for the type J. Only a few percent of blocks were noted among all cases classified into this category. This type has the lowest frequency of blocks in comparison to all analysed jet stream patterns (Fig. 6).

The K jet divides Europe into cooler, eastern part and warmer, western region. Transition zone between both regions is situated along 15–20° E. Warm weather is connected with anticyclone which develops in the crest of the ridge, between the British Isles and Scandinavia. Slightly shifted to the east, over the Baltic Straits, the centre of descending motions is situated. Eastern Europe experiences the cold advection of polar-maritime air that is steered by the cyclone situated over north-western Russia (Fig. 7).

The main feature of the L type is a strong subtropical jet situated over northern Africa. The response of vertical circulation to upper level divergence associated with delta region is distinct in the area to the south of the Black Sea. Mean value of vertical velocity reaches here $-0.1\,\mathrm{Pa\,s^{-1}}$. Circulation conditions over the major part of Europe are shaped by an upper anticyclone situated over central Europe. The position of this blocking high in the whole class oscillates between 10 and 30° E. At the sea-level, pressure field forms the wedge of Azores high extended towards central and eastern Europe. The interior of the European continent experiences weak thermal advections from various directions. Only slight increase of temperature over northern Europe and slight cooling over the Mediterranean is observed (Fig. 7).

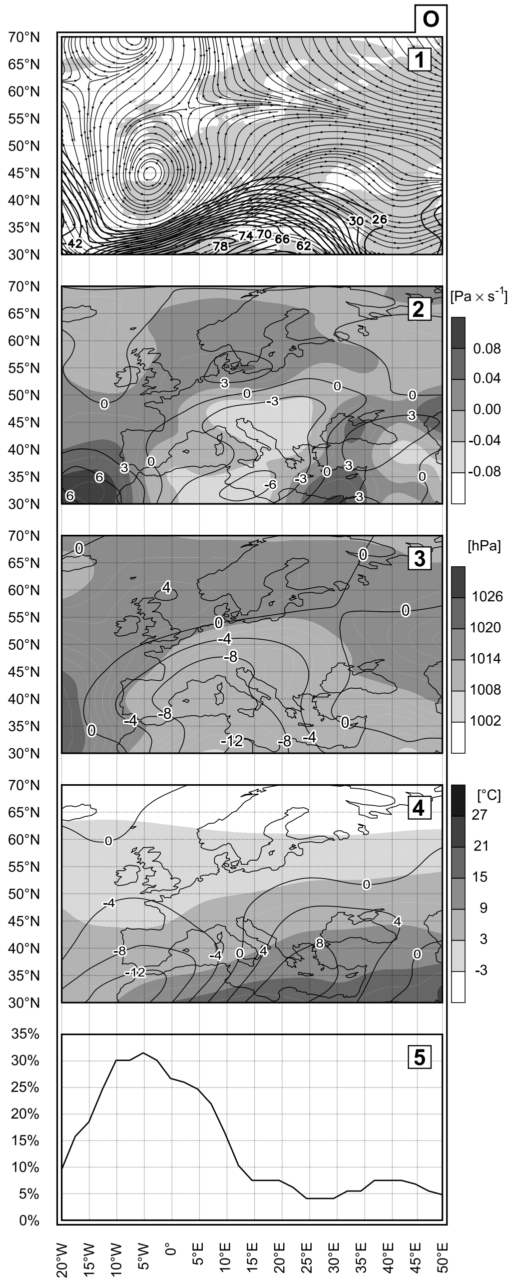

Fig. 9. Same as Fig. 2 except for type O

During the domination of the M pattern the low-level air flow over south-western and central Europe is directed generally from south-west to north-east. Such warm thermal advection is steered by cyclone centred south to Ireland and anticyclonic wedge spreading from the central Mediterranean to eastern Europe. Most significant temperature rise is observed over Poland. Both pressure systems pronounce the character of atmospheric blocks. They are relatively frequent in the belt 25–30° E and between 20 and 10° W (Fig. 8).

Type N is an example of omega block with upper anticyclone located north of the British Isles. The centre of low-level high is situated slightly to south-east in relation to the circulation aloft. Significant downward motions at 500 hPa level cover the North Sea and the Baltic region.

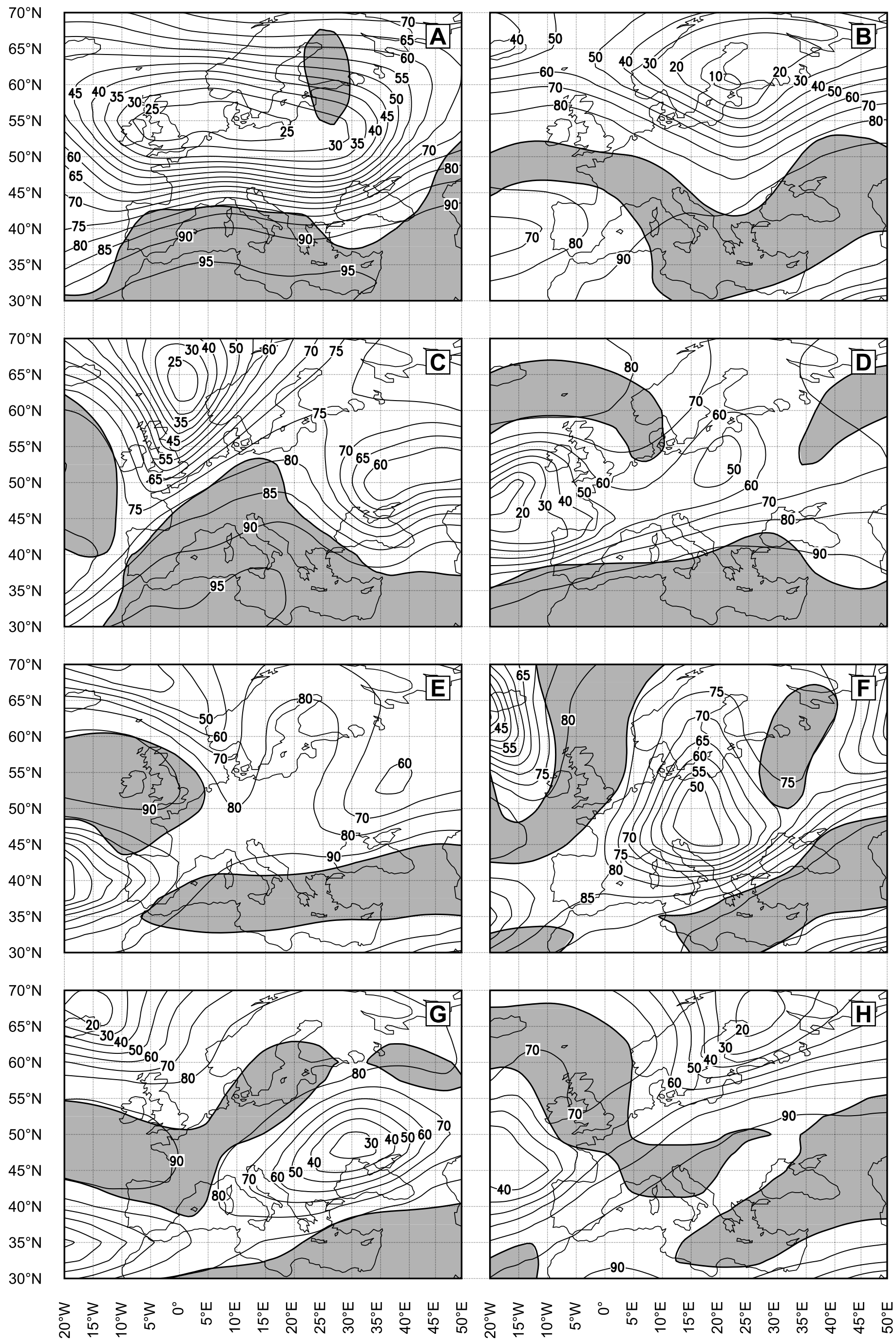

Fig. 10. Distribution of directional steadiness of wind vector in a given jet stream class [%]. Jet structure, i.e. the region where the wind speed exceeds 26 ms^{-1}, is shaded

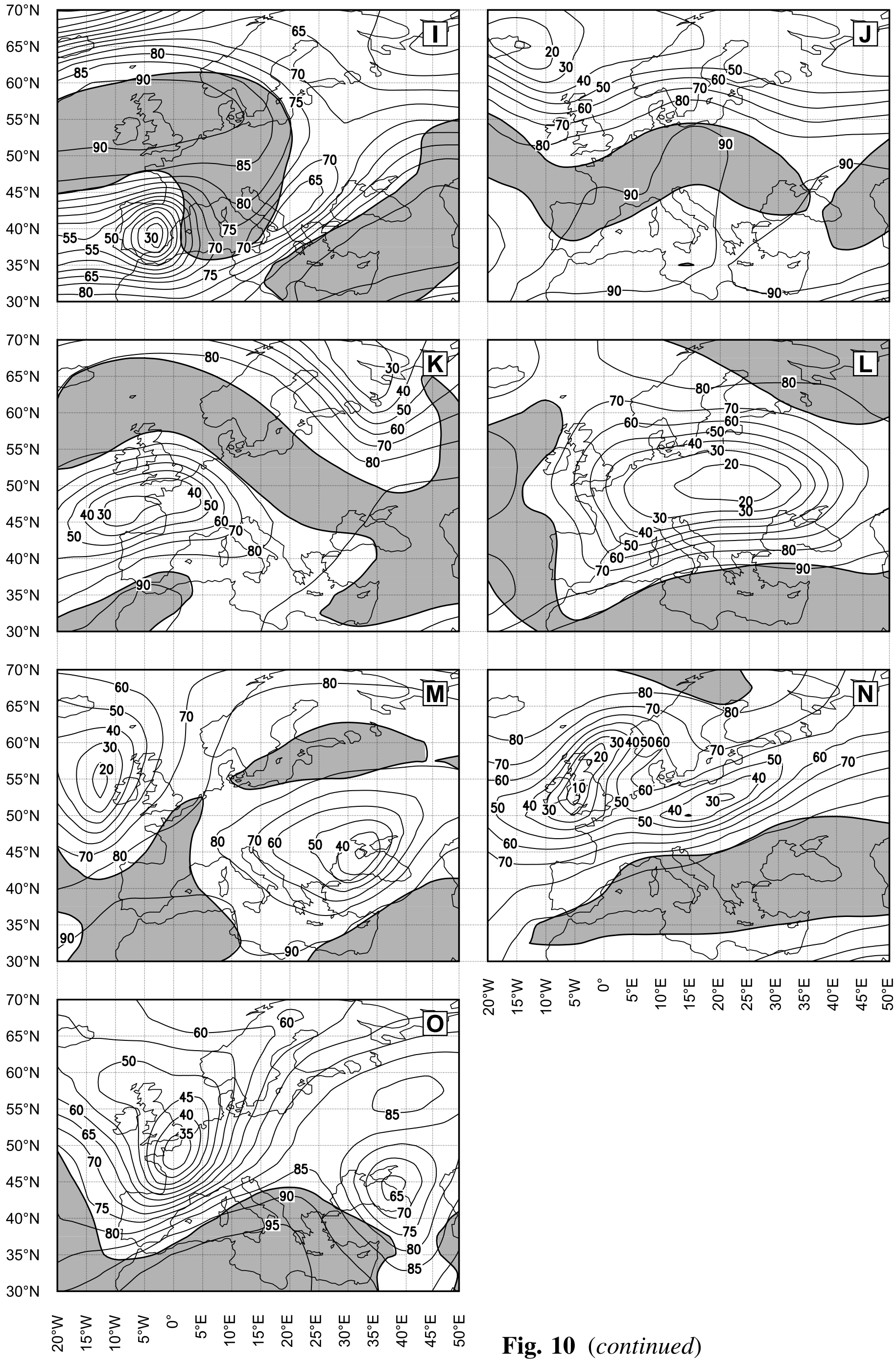

Fig. 10 (*continued*)

Because of northerly advection along the east side of the ridge temperature is usually below normal in south-central Europe (Fig. 8).

The last, O type, is characterised by a well developed block observed to the west of the Prime Meridian. In this region, intense flow of cold air from the north is observed aloft. On their way southward, air masses are forced to descend. Maximum sinking is observed in the proximity of the left entrance of the subtropical jet streak. Northern advection reaches African coast and brings about significant temperature drop. Increased thermal contrasts between south-western Europe and Africa intensify the subtropical jet stream. The wind speed within the jet streak is the highest compared to all 15 categories and reaches $80\,\mathrm{ms}^{-1}$. South-eastern Europe experiences warm weather associated with the east sector of the low centred over the Alps and the Apennine Peninsula (Fig. 9).

4. Directional steadiness of wind vectors within the jet stream classes

To check the consistency of jet stream patterns, directional steadiness of wind vectors at each grid point and for all class members was calculated (Fig. 10). Minimum, average and maximum values of this parameter characteristic for jet stream structure were evaluated and presented in Table 2.

Spatially averaged directional steadiness for the regions with wind speed exceeding $26\,\mathrm{ms}^{-1}$ is quite high, from 84.6 to 93.6%. The lowest minimum values (30–50%) characterise jetlets (e.g. type A) and jet finger structures (e.g. type K). High directional stability is the feature of zonal jets (e.g. type J, minimum $P = 79.1\%$) and also of the patterns with dominant subtropical jet and lack of polar one (e.g. type N, with regard to both, its minimum and average P). Subtropical jets are characterised by the highest directional stability – values 97–98% refer to jet streaks situated over northern Africa. To sum up, it should be stated that the spatial distribution of directional steadiness corresponds to the structure of selected jets and the values observed within the area of the jet are similar to those describing the stability of the warm westerly advection over Europe during winter season (Degirmendžić, 2004).

5. Seasonal and long-term changes of the jet stream types

The frequency of classified patterns and the dates of the occurrence of the type defining classes are shown in Table 1. The A pattern occurs in 11.4% of all days, whereas the O is observed only in 1.6% of the sample. August is characterised by the greatest variability of jet stream shape. The cumulative relative frequency of all 15 types equals only 52.5% during this month. It means that wind field is considerably different from the patterns classified every two days on average. In April types A–O represent the highest percentage of all cases – 73.7. Generally, the circulation at 200 hPa level is characterised by greater recurrence of selected types in spring (Apr–May) than in summer (Jun–Sep). In April and May patterns A, C and D are the most frequent. Their frequency varies from 25% for the A pattern in April to ca. 7% for the D pattern in May. The maximum number of days with the A type, equal to 21, was observed in May 1981 (Table 3). Two other types (C and D) occurred 15 and 13 times at most, respectively. In June, types A and C still dominate, but the third most frequent is pattern B, which prevails during summer. In July and August types E, J and H are also very common.

Table 1. Relative frequency of 15 most frequent jet stream types [%] and the date of days defining classes in the period 1950–2001

Type	Date	Apr	May	Jun	Jul	Aug	Sep	Apr–Sep	Cum
A	14.04.1980	25.4	23.0	13.1	2.2	1.8	3.1	11.4	11.4
B	14.07.1993	2.4	2.2	7.9	16.2	10.5	4.7	7.3	18.8
C	15.04.1999	12.1	11.2	8.7	2.6	2.6	3.4	6.8	25.5
D	24.05.1952	13.2	6.7	4.9	1.2	1.9	2.4	5.1	30.6
E	3.08.1961	0.5	0.6	4.2	7.6	6.8	5.0	4.1	34.7
F	12.09.1999	1.2	1.2	3.5	4.7	6.2	7.4	4.0	38.7
G	28.05.2000	2.5	5.0	5.6	1.1	1.4	4.6	3.4	42.1
H	30.08.1978	0.8	1.1	3.0	4.9	4.9	3.7	3.1	45.2
I	29.09.1996	1.0	1.6	2.0	2.4	3.5	7.4	3.0	48.1
J	2.08.1950	0.2	0.7	0.6	7.2	6.3	1.2	2.7	50.8
K	31.08.1987	0.7	0.4	2.6	2.6	2.2	5.4	2.3	53.2
L	9.04.1969	6.4	3.7	1.2	0.2	0.4	1.5	2.2	55.4
M	23.05.1950	2.4	5.1	2.9	0.4	0.4	1.0	2.0	57.4
N	25.08.1970	0.3	0.7	0.9	3.0	3.3	2.5	1.8	59.2
O	3.04.1964	4.6	4.0	0.7	0.0	0.0	0.0	1.6	60.8

Cum cumulative relative frequency

Table 2. Minimum, average and maximum values of the directional steadiness [%] calculated for the jet stream area delimited by $26\,ms^{-1}$ isotach

Type	Min	Average	Max
A	28.3	88.0	96.6
B	78.4	92.1	96.9
C	73.1	89.3	96.4
D	64.9	88.0	96.7
E	72.0	92.6	96.5
F	71.7	86.6	97.5
G	76.5	90.2	96.7
H	63.9	84.6	96.2
I	56.5	88.4	96.6
J	79.1	89.1	95.9
K	49.1	88.9	97.6
L	64.3	86.1	98.2
M	72.1	89.7	96.8
N	83.1	93.6	96.6
O	77.4	91.5	97.7

Mean frequency of 3% characterises type H in June, coming in eight position. By comparison, this pattern occurred 12 times in 1984 during this month (40%). Similar maximum frequency is associated with types A and C – the most common in June with regard to their mean relative frequencies. Type F represents blocking pattern in central Europe that is relatively frequent in summer. In July and August it occurs once per 20 days on average, but may reach 33% at most. In September the differences in frequencies of the classified types are relatively small. Patterns F, I and K are slightly more frequent. Among them, type K is characterised by the highest maximum frequency – 11 days with this pattern was noted in year 1959. The occurrence of classes L and M, which are associated with frequent blocks over central Europe, is limited to Apr–May season (Table 1). Type N with omega block over the Atlantic is present mainly from July to September. The last classified pattern – O, which pronounces characteristic feature of block in eastern Atlantic, shapes circulation only in spring. It is worth emphasising that the maximum frequency of this type in May equals 10 days, which gives it 4^{th} score. As regards its mean frequency, only five types are more frequent.

The persistence of selected jet types, expressed in the number of consecutive days grouped into a given class, is not very high. The longest mean duration (3.3 days) characterises pattern A in May (Table 3). Also the maximum duration gives type A first position – in May 1981 this pattern lasted incessantly 21 days. It is almost twice as long as pattern C, situated on the second position as far as the maximum duration is concerned (Table 3). Only five patterns have mean duration time longer than two days: pattern A from April to June and in August, pattern B from June to August, pattern C from May to June, pattern D from April to May and pattern H in June. Out of them, the first four types (A–D) lasted longer than one week. High maximum duration is

Table 3. Maximum number of days with jet stream (T) patterns (n_{max}), average duration time [days] (d_{ave}) and maximum duration of jet stream types [days] (d_{max}) in the period 1950–2001

T	Apr			May			Jun			Jul			Aug			Sep			Apr–Sep		
	n_{max}	d_{ave}	d_{max}	n_{max}	d_{ave}	d_{max}	n_{max}	d_{ave}	d_{max}	n_{max}	d_{ave}	d_{max}	n_{max}	d_{ave}	d_{max}	n_{max}	d_{ave}	d_{max}	n_{max}	d_{ave}	d_{max}
A	19	2.74	10	21	3.33	21	13	2.49	11	4	1.41	3	5	2.14	4	4	1.45	3	43	2.65	21
B	6	1.80	5	5	1.94	5	11	2.31	7	14	2.74	9	8	2.28	7	6	1.83	4	25	2.32	9
C	13	1.88	6	15	2.03	11	11	2.25	11	5	1.52	3	5	1.35	4	6	1.63	5	22	1.89	11
D	13	2.17	8	11	2.02	6	6	1.77	4	4	1.50	4	5	1.67	5	8	1.55	8	21	1.94	8
E	2	1.14	2	2	1.11	2	5	1.60	5	9	1.47	6	10	1.67	5	8	1.49	5	17	1.53	6
F	3	1.36	3	3	1.46	3	7	1.69	7	11	1.80	13	11	1.60	6	9	1.69	5	17	1.65	13
G	5	1.33	3	6	1.88	6	9	1.80	7	3	1.19	2	4	1.28	3	7	1.43	3	16	1.57	7
H	3	1.44	3	3	1.38	3	12	2.04	6	7	1.67	5	6	1.63	5	5	1.32	2	24	1.60	6
I	3	1.27	3	3	1.37	3	4	1.55	3	4	1.32	3	5	1.44	4	9	1.82	4	19	1.54	4
J	2	1.00	1	2	1.20	2	2	1.00	1	10	1.84	6	10	1.62	6	4	1.38	3	16	1.62	6
K	3	1.22	2	2	1.17	2	7	1.46	4	7	1.62	5	8	1.89	6	11	1.95	6	17	1.68	6
L	8	1.76	5	5	1.40	5	6	1.80	6	2	1.50	2	1	1.00	1	4	1.24	2	11	1.54	6
M	6	1.40	4	9	1.80	9	5	1.74	4	2	1.50	2	3	1.75	3	4	1.50	3	12	1.66	9
N	1	1.00	1	2	1.20	2	4	1.27	2	5	1.81	5	7	1.54	4	6	1.42	6	14	1.50	6
O	5	1.49	4	10	1.68	5	3	1.25	3	0	0	0	0	0	0	0	0	0	11	1.55	5

Table 4. Trend coefficients of jet types (T) frequency [days (50 years)$^{-1}$] (a_n) and mean duration of jet types [days (50 years)$^{-1}$] (a_d) in the period 1950–2001. Trends were calculated on the basis of 52-element records unless different number is given in brackets. Coefficients significant at 0.05 level, according to F test, are bolded

T	Apr		May		Jun		Jul		Aug		Sep		Apr–Sep	
	a_n	a_d	a_n	a_d	a_n	a_d	a_n	a_d	a_n	a_d	a_n	a_d	a_n	a_d
A	−0.90	−0.57 (50)	2.52	1.72 (47)	−0.44	−0.22 (47)	−0.75	−0.64 (18)	−0.63	−0.68 (13)	−0.07	0.22 (25)	−0.28	0.45
B	−0.44	−0.96 (15)	−0.54	−1.02 (16)	2.09	0.41 (34)	2.05	0.08 (43)	−0.60	0.32 (43)	0.52	0.26 (32)	3.09	0.23
C	1.90	0.24 (47)	0.02	0.77 (46)	0.03	−0.27 (35)	0.48	**1.09** (22)	**−1.47**	−0.17 (21)	−0.59	−0.26 (22)	0.36	0.26
D	−1.05	−0.97 (44)	−0.72	−0.37 (31)	−0.33	0.34 (28)	−0.43	−1.08 (10)	0.41	−0.23 (16)	0.43	1.60 (19)	−1.69	−0.43
E	0.10	−0.06 (7)	0.21	0.65 (9)	0.36	−1.03 (28)	−0.93	−0.46 (43)	−1.06	0.45 (40)	−0.26	0.43 (32)	−1.57	0.01
F	−0.05	−0.31 (12)	−0.52	−1.48 (12)	−0.90	−0.40 (24)	0.20	0.88 (30)	−0.28	−0.32 (37)	−0.72	0.44 (35)	−2.27	0.37 (51)
G	**1.21**	0.75 (22)	−0.64	0.27 (28)	−1.12	−0.78 (32)	**0.67**	0.22 (12)	**−1.21**	−0.01 (14)	**−1.80**	−0.23 (30)	−2.88	−0.16 (50)
H	0.01	−0.73 (8)	0.19	0.30 (12)	0.83	1.10 (16)	0.72	−0.50 (32)	1.31	0.12 (32)	0.08	−0.05 (25)	3.15	0.17 (48)
I	0.42	1.00 (9)	0.43	0.44 (15)	0.07	−0.10 (15)	0.66	−0.20 (24)	0.44	−0.13 (27)	−0.76	0.07 (30)	1.26	−0.04
J	0.26	– (1)	−0.31	−0.72 (10)	**0.67**	0.00 (7)	−0.14	−0.38 (34)	−2.01	0.12 (33)	0.36	0.33 (11)	−1.17	**−0.60** (47)
K	0.50	0.39 (8)	**0.38**	0.37 (6)	0.14	0.06 (21)	−0.20	1.13 (16)	**1.31**	0.63 (14)	−0.03	−0.10 (24)	2.11	0.49 (44)
L	−0.51	−0.12 (37)	−0.54	−0.09 (28)	−0.53	1.13 (8)	0.03	−2.50 (2)	**0.35**	0.00 (6)	0.11	0.14 (13)	−1.08	−0.38 (46)
M	0.81	−0.49 (21)	−0.60	−0.93 (30)	−0.04	0.62 (24)	0.28	0.88 (4)	−0.31	−3.11 (4)	0.10	0.07 (9)	0.24	−0.79 (44)
N	−0.01	0.00 (4)	0.09	0.13 (8)	0.07	0.23 (8)	−0.51	−0.84 (22)	0.06	−0.04 (20)	0.67	−0.02 (21)	0.37	−0.23c (42)
O	0.69	0.44 (32)	−0.56	−0.20 (24)	**−0.52**	−1.57 (8)	–	– (0)	–	– (0)	–	– (0)	−0.40	0.16 (47)

Table 5. Average day-to-day changes of selected jet stream types, expressed as the mean of vector correlation calculated for the consecutive wind fields within each category during warm half-year in the period 1950–2000 ($\rho_\nu{}^2$ and trend coefficients of this statistic per 50 years (Δ). *N* number of warm half-year periods used for trend calculation. Significant values, according to the F-test, are bolded

	Jet stream type														
	A	B	C	D	E	F	G	H	I	J	K	L	M	N	O
$\rho_\nu{}^2$	1.38	1.3	1.38	1.39	1.18	1.27	1.23	1.29	1.16	1.21	1.18	1.29	1.31	1.27	1.31
Δ	−0.05	0.05	−0.05	**−0.14**	0.03	0.00	−0.07	−0.15	−0.1	0.06	0.05	**−0.21**	−0.18	−0.2	−0.11
N	51	49	48	46	41	46	40	33	43	34	28	31	33	27	24

observed also in the case of blocking types F (13 days in July 1994) and M (9 days in May 1969). There are also several jet stream types lasting one day: pattern J in April and June, L in August and N in April. They are also marked by very low mean frequency of occurrence, below 1%.

It is worth underlining that statistically significant trend in frequency of at least one jet type is observed in each calendar month (Table 4). However, the trend coefficients are relatively small, in the order of 1–2 days per 50 years. In April, the increase in the type G frequency, which is propitious for fair weather in eastern Europe, is observed. Simultaneously, the mean duration of this pattern prolonged by about 0.75 day in 50-year period. In May, weak but statistically significant upward trend in the frequency of the K pattern was found. In June, the number of occurrence of type J increased slightly while pattern O became less frequent. As both types generate cold advection in western and south-western Europe their net impact on air temperature may not be detectable. In July, pattern G, which brings the cool waves in western Europe, occurred slightly more often. The persistence of this pattern also increased, but this effect is statistically insignificant. In July, an appreciable rise in mean duration of pattern C which strengthens the north-western advection over western Europe is noted. In August, the character of the upper tropospheric circulation considerably changed. The number of types C and G diminished, which may result in less frequent cold advection over western Europe. At the same time, the frequency of patterns K and L, which are responsible for higher than normal temperature in western Europe, was on the increase. Relatively distinct decreasing trend of pattern G was observed also in September.

Among the long-term tendencies of day-to-day wind changes, negative tendencies prevail. It means that the average coefficient of vector correlation calculated between consecutive wind fields reaches lower values. 10 out of 15 patterns are marked by negative tendencies, but only in two cases (patterns D and L) they are statistically significant (Table 5). These trends may indicate slight enhancement of the upper tropospheric circulation dynamics.

6. Conclusions

It seems that Lund's method, which uses vector correlation instead of the linear Pearson coefficient, constitutes easy to use statistical tool of credible quality, by means of which the most frequent types of vector fields can be selected. Jet stream classes analysed in this paper are characterised by high internal consistency – directional steadiness of wind vectors computed for the jet stream region within a given class is about 80–90%. The major drawback of Lund's technique is excessive number of small classes (<1.5% of the total sample). The 15 selected jet stream classes grouped 60.8% of the total sample. For comparison, Bischoff and Vargas (2003) left 15% of fields unclassified, Lund (1963) about 10%, Paegle and Kierulff (1974) did not clustered 12% of fields. Their residual samples were considerably smaller. It is due to the fact that the area of their investigation was also considerably smaller and the period of time shorter than in current analysis.

The selected jet types were analysed with respect to their associated sea-level pressure, vertical velocity and temperature fields. Types F, M and G seem to substantially contribute to the warming up of central Europe. Types E, C and G are responsible for considerable cooling in the west. Types I, D, B, H, K and N pronounce reversed thermal effect, which is characterised by warm advection in western Europe. Additionally, types B and H generate cold waves in central Europe.

Several jet stream patterns revealed distinct seasonal variation in frequency and duration time. Types A, C and D, which cause major temperature changes in western Europe, dominate in spring with maximum duration reaching 21 days during this season. These are meridional types of circulation. The last, O type, occurs only in Apr–Jun period. In summer, patterns B, E and J are very common. While they are present, zonal flow is enhanced. However, blocking type F is also relatively frequent in this season. It has the highest maximum persistence (13 days) in comparison to any other summer patterns. In September types F, I and K are slightly more frequent.

Changes in the frequency and duration of the classified jet stream types are rather minor. Although some of the trend coefficients exceed 0.05 level of statistical significance (α), the number of positive test results with respect to all tests (15 patterns multiplied by 6 months) does not differ much from α. It leads to the conclusion that all positive results may be the errors of the first kind. Despite their small magnitude, some tendencies may be reflected in the specific changes of the environment. For example, the increase in the frequency of type G in April may be partially responsible for the early spring warming that has been observed in central and north-eastern Europe recently (Kożuchowski and Żmudzka, 2001; Jaagus, 2006). In August, the frequency of types C and G, which cause cooling in western Europe, decreases. Type K, which warms up this region, occurs more often. These three tendencies contribute to the warming of western Europe and cooling of the eastern part of the continent. Negative trend in the frequency of type G is observed in September. It may be reflected in less frequent cool waves in western Europe. Indeed, during Aug–Sep period the rise in temperature was observed in the west (Klein Tank et al., 2002), while eastern Europe experienced decline in temperature. Negative trends are reported for Estonia (Jaagus, 2006), Lithuania (Bukantis and Rimkus, 2005) and western Russia (Klein Tank et al., 2002). The transitional zone between the regions with opposite tendencies is situated in central Europe. For instance, in Poland, trend in the air temperature in Aug–Sep period is close to 0 (Degirmendžić et al., 2004).

Finally, it is worth noting that day-to-day changes of jet spatial structure became greater for the most of patterns (10 out of 15). It may suggest moderate rise in the complexity of upper level circulation. However, this tendency is not associated with the shortening of the duration of selected jet stream types.

Acknowledgments

Special thanks to Tomasz Minkiewicz for his technical assistance. Our sincerest gratitude goes to Kamila Witczak for improving our English. We would like to thank also anonymous referees for suggesting changes that strengthened the exposition of this paper.

References

Bischoff SA, Vargas WM (2003) The 500 and 1000 hPa weather type circulations and their relationship with some extreme climatic conditions over southern South America. Int J Climatol 23: 541–556

Bolek C, Degirmendžić J (2004) Temperature fields clustering based on competitive Kohonen rule with degrading conscience. Proc "Artificial Intelligence in Control and Management" conference, September 14th, Łódź, Poland, pp 67–77

Breaker LC, Gemmill WH, Crosby DS (1994) The application of a technique for vector correlation to problems in meteorology and climatology. J Appl Meteor 33: 1354–1365

Budziszewska E (1977) Troposferyczne prądy strumieniowe nad Polską, ich długotrwałość i rozkład częstości (Tropospheric jet streams above Poland, their derivation and frequency). Prace i studia Instytutu Geograficznego UW, ser. klimatologia 9: 197–202

Bukantis A, Rimkus E (2005) Lithuanian climate in the 18th–21st centuries. Acta Zoologica Lithuanica 15 (in print)

Crosby DS, Breaker LC, Gemmill WH (1993) A proposed definition for vector correlation in geophysics: theory and application. J Atmos Oceanic Technol 10: 355–367

Degirmendžić J (2004) Fale termiczne nad Polską w zimie w zależności od pola wiatru w Europie (Thermal waves in Poland during winter in relation to the wind field in Europe). Przegląd Geofizyczny 1–2: 11–23

Degirmendžić J, Kożuchowski K, Żmudzka E (2004) Changes of air temperature and precipitation in Poland in the period 1951–2000 and their relationship to atmospheric circulation. Int J Climatol 24: 291–310

Erdogmus F (1992) Steadinees of the upper winds up to 100 hPa over Turkey between 1970 and 1984. Il Nuovo Cimento. C: Geophysics and Space Physics 15C(1): 107–110

Glickman TS (ed) (2000) Glossary of meteorology, 2nd edn. American Meteorological Society, 850 pp

Hardy DM, Walton JJ (1978) Principal components analysis of vector wind measurements. J Appl Meteor 17: 1153–1162
Huth R (1996) An intercomparison of computer-assisted circulation classification methods. Int J Climatol 16: 893–922
Jaagus J (2006) Climatic changes in Estonia during the second half of the 20th century in relationship with changes in large-scale atmospheric circulation. Theor Appl Climatol 83: 77–88
Kalkstein L, Tan G, Skindlov J (1987) An evaluation of three clustering procedures for use in synoptic climatological classification. J Climate Appl Meteor 26: 717–730
Kalnay E, Kanamitsu M, Kistler R, Collins W, Deaven D, Gandin L, Iredell M, Saha S, White G, Woollen J, Zhu Y, Chelliah M, Ebisuzaki W, Higgins W, Janowiak J, Mo KC, Ropelewski C, Wang J, Leetmaa A, Reynolds E, Jenne R, Joseph D (1996) The NCEP/NCAR 40-year reanalysis project. Bull Amer Meteor Soc 77: 437–471
Kasper M (1976) Ein Beitrag zur Klimatologie der Strahlströme über dem Gebiet der DDR (Contribution to the climatology of the jet streams over the GDR). Zeitschrift für Meteorologie 6: 330–338
Kasper M (1978) Strahlstromcharakteristika und ihr Zusammenhang mit bestimmten Wetterelementen – eine statistisch-methodische Untersuchung (Jet-stream characteristics and their relationships to selected weather elements, a statistical and stochastic study). Zeitschrift für Meteorologie 6: 311–318
Kaufmann RK, Snell SE, Gopal S, Dezzani R (1999) The significance of synoptic patterns identified by the Kirchhofer technique: a Monte Carlo Approach. Int J Climatol 19: 619–626
Klein Tank AMG, Wijngaard J, van Engelen A (2002) Climate of Europe. European Climate Assessment (ECA), de Bilt, Netherlands, 36 pp
Kożuchowski K, Żmudzka E (2001) Ocieplenie w Polsce: skala i przebieg sezonowy zmian temperatury powietrza w drugiej połowie XX wieku (Warming in Poland: scale and seasonal distribution of air temperature changes in the second half of the 20th century). Przegląd Geofizyczny 1–2: 81–90
Legler DM (1983) Empirical orthogonal function analysis of wind vectors over the tropical Pacific region. Bull Amer Meteor Soc 64: 234–241
Lejenäs H, Økland H (1983) Characteristics of Northern Hemisphere blocking as determined from a long time series of observational data. Tellus 35A: 350–362
Lund IA (1963) Map-pattern classification by statistical methods. J Appl Meteor 16: 20–33
Malnar-Tomic V (1995) Analiza jakog visinskog vjetra i tropopauze iznad sjeverozapadne Hrvatske i zapadne B I H (An analysis of strong winds aloft and of the tropopause above NW Croatia and western Bosnia and Herzegovina). Hrvatski Meteorološki Časopis 30: 71–77
Overland JE, Hiester TR (1980) Development of a synoptic climatology for the Northeast gulf of Alaska. J Appl Meteor 19: 1–14
Paegle JN, Kierulff LP (1974) Synoptic climatology of 500-mb winter flow types. J Appl Meteor 13: 205–213
Panofsky HA, Brier GW (1958) Some applications of statistics to meteorology. Pennsylvania State University Press, 226 pp
Reap RM (1994) Analysis and prediction of lightning strike distributions associated with synoptic map types over Florida. Mon Wea Rev 122: 1698–1715
Reiter ER (1963) Jet stream meteorology. ■: University of Chicago Press, 510 pp
Richman MB (1981) Obliquely rotated principal components: an improved meteorological map typing technique? J Appl Meteor 20: 1145–1159
Rose SF, Hobbs PV, Locatelli JD, Stoelinga MT (2004) A 10-yr climatology relating the locations of reported tornadoes to the quadrants of upper-level jet streaks. Weather Forecast 19: 301–309
Shutts GJ (1987) Persistent anomalous circulation and blocking. Meteor Mag 116: 116–124
Singh MS (1980) Tropspheric structure and jet streams over the Middle East in winter. Mausam 31: 241–246
Trenberth KE (1991) Storm tracks in the Southern Hemisphere. J Atmos Sci 48: 2159–2178
Uccellini LW, Kocin PJ, Petersen RA, Wash CH, Brill KF (1984) The Presidents' Day Cyclone of 18–19 February 1979: Synoptic Overwiev and Analysis of the Subtropical Jet streak influencing the pre-cyclogenetic period. Mon Wea Rev 112: 31–55
Uccellini LW, Kocin PJ (1987) The interaction of jet streak circulations during heavy snow events along the east coast of the United States. Weather Forecast 1: 289–308
von Storch H, Zwiers FW (1999) Statistical analysis in climate research. ■: Cambridge University Press, 484 pp
Wibig J (2001) Wpływ cyrkulacji atmosferycznej na rozkład przestrzenny anomalii temperatury i opadów w Europie (Impact of atmospheric circulation on spatial distribution of the air temperature and precipitation anomalies in Europe). Wydawnictwo UŁ, 208 pp
Ziv B, Paldor N (1999) The divergence fields associated with time-dependent jet streams. J Atmos Sci 56: 1842–1857

Authors' addresses: Jan Degirmendžić (e-mail: jandegir@geo.uni.lodz.pl), Department of Environmental Dynamics and Bioclimatology, University of Łódź, ul. Narutowicza 88, 90–139 Łódź, Poland; Joanna Wibig, Department of Meteorology and Climatology, University of Łódź, Łódź, Poland.